

# A myosin II mutation uncouples ATPase activity from motility and shortens step size

Coleen T. Murphy, Ronald S. Rock and James A. Spudich\*

Departments of Biochemistry and Developmental Biology, Stanford University School of Medicine, Stanford, California 94305, USA  
\*e-mail: jspudich@cmgm.stanford.edu

**It is thought that Switch II of myosin, kinesin and G proteins has an important function in relating nucleotide state to protein conformation. Here we examine a myosin mutant containing an S456L substitution in the Switch II region. In this protein, mechanical activity is uncoupled from the chemical energy of ATP hydrolysis so that its gliding velocity on actin filaments is only one-tenth of that of the wild type. The mutant spends longer in the strongly bound state and exhibits a shorter step size, which together account for the reduction in *in vitro* velocity. This is the first single point mutation in myosin that has been found to affect step size.**

The ability to convert chemical energy into mechanical movement is the essence of a molecular motor, yet the mechanism behind this coupling is still not well understood. Myosin, an actin-based motor that contributes to such vital functions as cell division, vesicle transport and muscular contraction, couples ATP hydrolysis to motility. Myosin hydrolyses ATP in the absence of actin, and phosphate release is triggered by actin binding (Fig. 1). The force-generating stroke, theoretically a lever-arm rotation of the light-chain-binding region, is thought to occur upon release of phosphate<sup>1</sup>. ADP then dissociates from the actin-bound myosin and ATP binds, causing actin to dissociate and the cycle to begin again. A key point of this model is that unnecessary ATP consumption is prevented by linking phosphate release, which is triggered by strong actin binding, to a conformational change of the lever arm; thus, ATPase activity is tightly coupled to motility. Here we describe a single point mutant of *Dictyostelium* myosin II, S456L, that exhibits an increased rate of phosphate release in the absence of actin, slowed release of actomyosin ADP, and reduced step size. The combination of these kinetic and mechanical defects causes uncoupling of its normal actin-activated ATPase activity from a normal stroke, resulting in reduced motility.

The most conserved regions of myosin are those that surround the nucleotide pocket, including the P-loop and the Switch I and II loops (Fig. 2a); these sequences are also conserved in kinesins and G proteins<sup>2</sup>. The conserved sequence DIXGFE (residues 454–459 of *Dictyostelium* myosin II) comprise the myosin Switch II region<sup>3</sup>. In crystallization studies of *Dictyostelium* myosin II, the Switch II loop has been shown to move >3 Å between the putative ATP state and the putative ADP–P<sub>i</sub> state (ADP–BeF<sub>3</sub> and ADP–AlF<sub>4</sub> myosin structures, respectively<sup>4</sup>). This movement corresponds to a rotation at residues I455 and G457, which induces a piston-like motion of the relay helix (Fig. 2a, b). The motion of the relay helix is transmitted both to the actin-binding site for myosin to affect actin affinity and to the lever arm to affect its angular position with respect to the catalytic domain. Mutagenic studies have shown that the conserved residues in this region are critical for hydrolysis and actin activation of ATPase activity<sup>5–10</sup>.

Myosin II is required at two stages of sorocarp development in *Dictyostelium*<sup>11</sup>, and the S456L mutation was first identified through its intermediate developmental phenotype<sup>5,12</sup>. Myosin II-null cells transformed with the S456L myosin plasmid are able to develop past the mound stage that is typical of myosin II-null mutants, but arrest in short, stubby, fingerlike projections rather than developing fully into sorocarps (Fig. 3a, b). Cells containing this myosin mutant also exhibit a growth-rate defect when grown in suspension, growing more slowly and saturating at one-third of the normal cell density.

To determine the cause of intermediate *in vivo* activity of S456L myosin, we purified the protein and analysed its biochemical characteristics<sup>5,13–17</sup>. The maximum actin-activated ATPase activity of S456L myosin<sup>18</sup> is similar to that of the wild type (Fig. 4a), but the

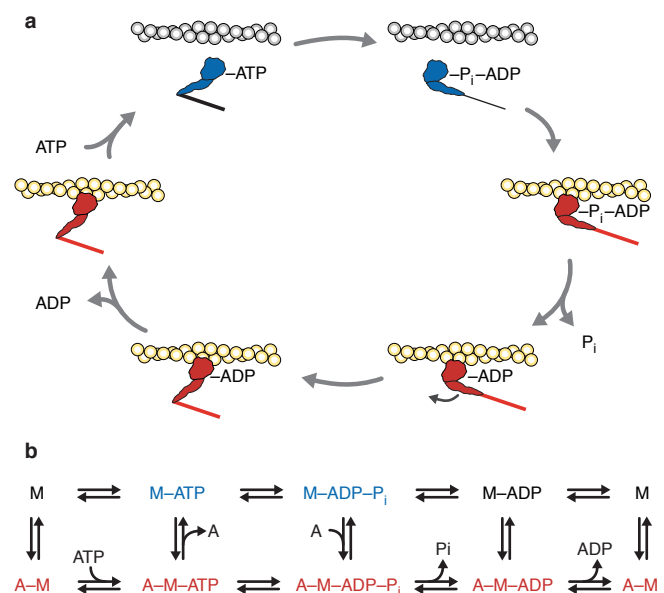


**Figure 1 The myosin ATPase cycle.** **a**, Schematic diagram showing the predominant states of the actin–myosin ATPase cycle and the presumed state of the lever arm in each state. Actin-bound states are represented in red; dissociated states are shown in blue. Myosin (M) binds to ATP, hydrolyses it to ADP–P<sub>i</sub> and releases the products in the absence of actin (**b**, upper line), but phosphate release is very slow. Actin (A) binding (red myosins in **a**, lower line in **b**) accelerates phosphate release, which is thought to precede the working stroke. ADP release is the slowest of the strongly bound rates, and is thought to limit velocity. Rebinding of ATP causes dissociation from actin and starts the cycle again.

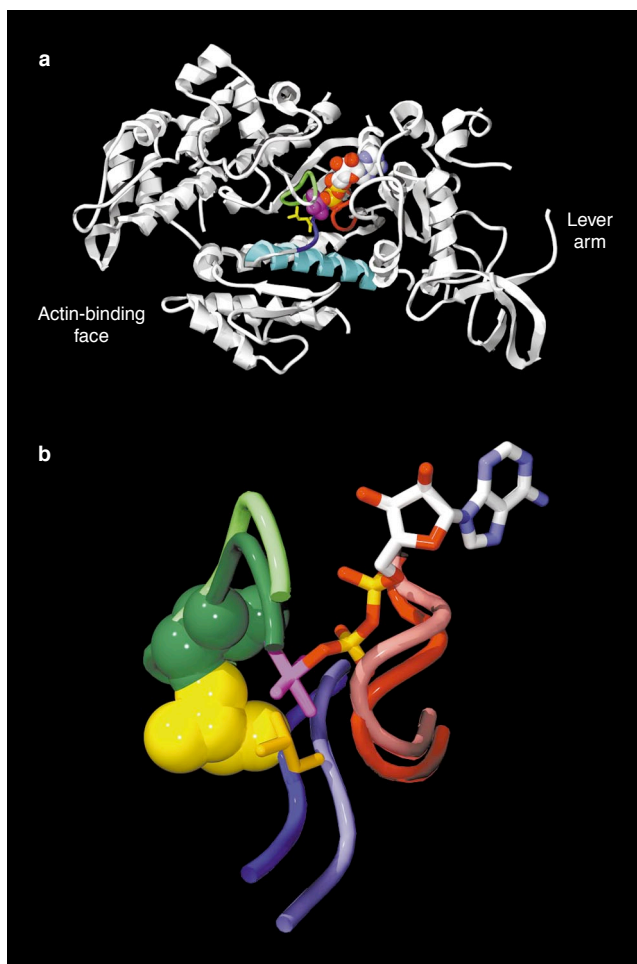


**Figure 2 Crystal structure of *Dictyostelium* myosin II catalytic domain.** The structure of the catalytic domain as resolved with ADP and aluminum fluoride<sup>4</sup> **a**, The nucleotide is represented in space-filling balls; phosphates are shown in yellow and aluminum fluoride in purple. The three conserved loops surround the  $\gamma$ -P<sub>i</sub> site — the P-loop (red), the Switch I loop (green) and the Switch II loop (blue). The S456L mutation in the Switch II loop is shown in yellow. The Switch II loop is connected to the relay helix (cyan). **b**, Energy-minimized model (Swiss-PDB Viewer) showing the mutant leucine residue at position 456 in the putative ATP (Mg-ADP-BeF<sub>3</sub> structure; pastel colors, yellow stick residue) and ADP-P<sub>i</sub> (Mg-ADP-AlF<sub>4</sub> structure; coloured as in **a**, yellow spacefill residue) states. In wild-type myosin, S456 is close to the Switch I loop in the ADP-P<sub>i</sub> state, but is sterically hindered (overlapping spheres) by S238 (green spacefill residue) when replaced by leucine.

mutant moves at only one-tenth of the speed of wild-type myosin in *in vitro* motility assays<sup>13,19,20</sup>, even at very high concentrations (Fig. 4b). This reduction in velocity is surprising when compared with the normal  $V_{max}$  of actin-activated ATPase activity, and indicates that ATPase activity has been uncoupled from normal actin translocation. In the absence of actin, S456L myosin releases phosphate, a product of ATP hydrolysis, at almost ten times the rate of wild-type myosin (Fig. 4a, c; see below). However, the rate of ATP hydrolysis by S456L myosin is the same as that by the wild type<sup>13,18</sup> (Table 1).

In a simple model of *in vitro* motility, velocity ( $v$ ) is expressed as  $v = d/t_s$ , where  $d$  represents step size and  $t_s$  is the time spent in the strongly bound state<sup>21</sup>. Mixing assays can be used as a measure of  $t_s$ . If the mutant were simply blocked in a strongly bound state, a great reduction in motility (equal to the velocity of the mutant) should

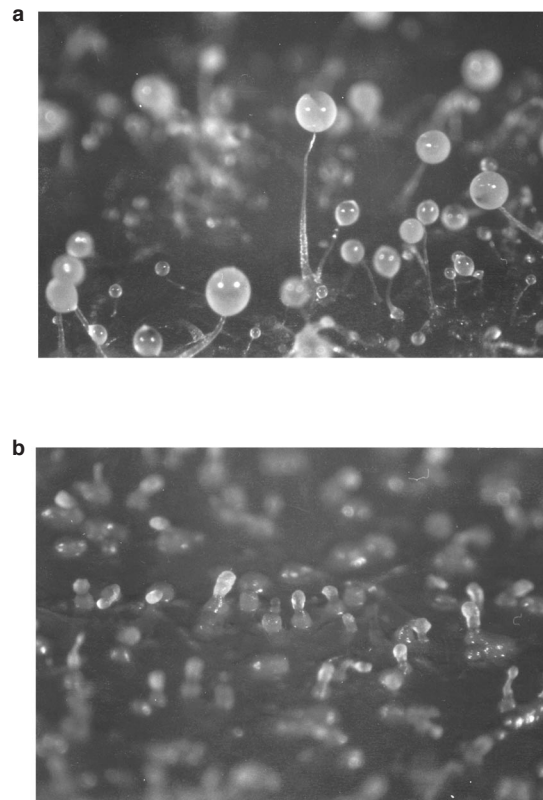


**Figure 3 S456L myosin exhibits *in vivo* defects.** Myosin II-null cells transformed with the S456L myosin plasmid are able to develop past the mound stage typical of myosin II-null mutants, but arrest in short, stubby, fingerlike projections (**b**) rather than developing fully into sorocarps, as in the wild type (**a**).

be observed when a small amount of mutant myosin is mixed with wild-type myosin in the *in vitro* motility assay. Conversely, if the mutant were blocked strictly in a weakly bound state, it should not significantly affect wild-type motility. When S456L myosin was mixed with wild-type myosin, the observed motility did not fit either of these models (Fig. 4d). The results of the mixing assay indicate that an increase in the time spent in the strongly bound state may contribute to the reduction in velocity, but that it cannot be the principal cause.

The time spent in the strongly bound state can be calculated, as it is determined by ADP release for vertebrate myosins<sup>22</sup> and by rates of both actin-myosin dissociation and ADP release for *Dictyostelium* myosin<sup>13</sup>. Like wild-type *Dictyostelium* myosin, S456L myosin binds to actin in the absence of ATP and is released when Mg<sup>2+</sup>-ATP is added. The affinity of the mutant for actin is similar to that of the wild type in the presence of ATP or ATP<sub>γ</sub>S in a co-sedimentation assay<sup>18</sup> (Table 1). Its rate of dissociation from phalloidin-stabilized actin by ATP was also normal (Table 1). However, in the presence of actin, S456L myosin releases mantADP at a little less than half the rate of wild-type myosin (Table 1). These results correlate well with those of the *in vitro* motility mixing assay — there was no change in the actin-myosin dissociation rate and ADP release was slowed, but to a degree that can account for no more than a twofold reduction in velocity, rather than the tenfold reduction observed.

According to the coupling model, ineffective communication of the hydrolysis state may result in reduced step size and velocity. We used the optical trap to measure the mean step size of wild-type and S456L myosin<sup>23–25</sup>, and found that the step size of the mutant

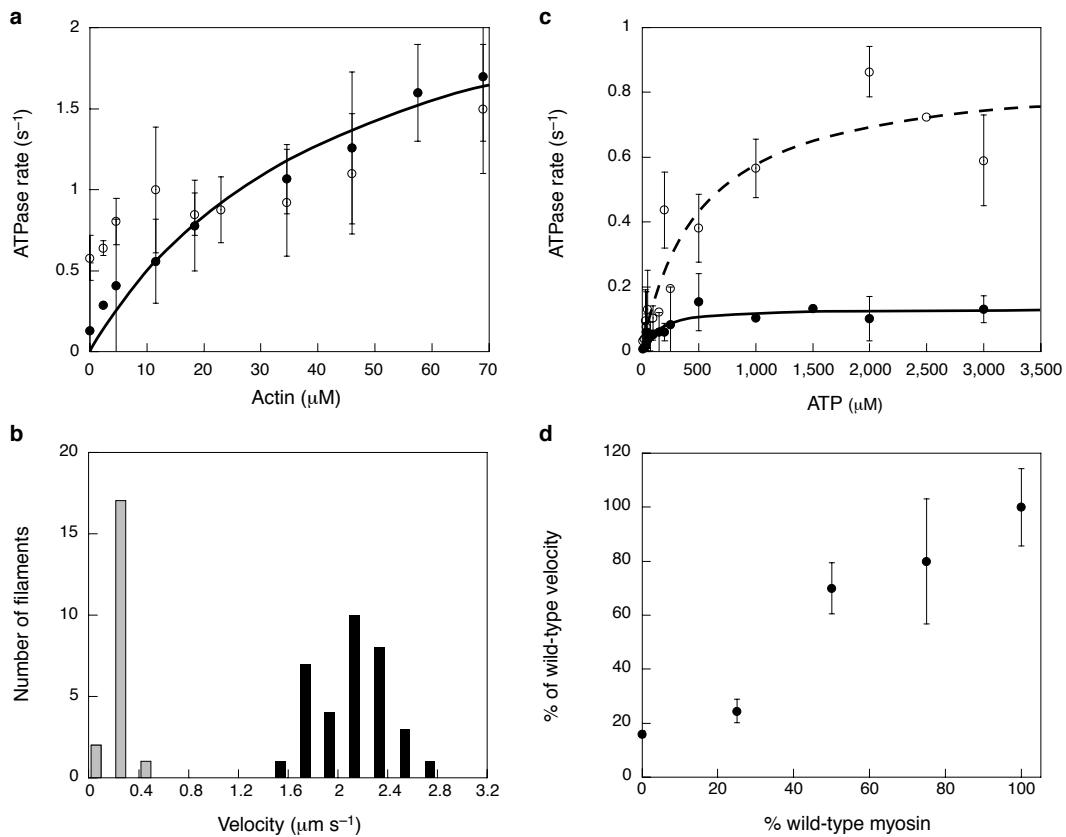


Figure 4 **ATPase activity and motility of S456L myosin.** **a**, ATPase activity as a function of actin concentration.  $V_{max}$  and  $K_m$  of the wild type are  $2.5 \pm 0.5 \text{ s}^{-1}$  and  $44.5 \pm 10 \text{ } \mu\text{M}$ , respectively. **b**, *In vitro* motility. The average velocity of S456L myosin is  $0.16 \pm 0.07 \text{ } \mu\text{m s}^{-1}$ , roughly one-tenth of that of the wild type ( $2.0 \pm 0.33 \text{ } \mu\text{m s}^{-1}$ ). Even at extremely high concentrations of S456L myosin (over ten times that of the wild type), its velocity does not exceed  $0.2 \text{ } \mu\text{m s}^{-1}$ . **c**, ATPase activity as a function of  $\text{Mg}^{2+}$ -ATP concentration. S456L myosin (open circles) exhibits a ten-

fold increase in basal ATPase activity (open circles;  $V_{max} = 1.0 \pm 0.1$  hydrolyses per s) relative to the wild type (filled circles;  $V_{max} = 0.1 \pm 0.03 \text{ s}^{-1}$ ). The  $K_m$  of S456L myosin for ATP is  $510 \pm 170 \text{ } \mu\text{M}$ , whereas the affinity of wild-type myosin for ATP is  $130 \pm 40 \text{ } \mu\text{M}$ . **d**, Mixing assays. Wild-type myosin was mixed with S456L myosin in ratios of 75:25, 50:50 and 25:75. Total myosin concentration was constant in the experiment shown here; similar results were obtained by adding mutant myosin to a fixed concentration of wild-type myosin.

was about one-fifth of that of the wild type ( $1.3 \pm 0.4 \text{ nm}$  and  $7.3 \pm 0.4 \text{ nm}$ , respectively; Fig. 5). For both mutant and wild-type myosins, the step size distribution could be fit by a single gaussian, with a width matching that of the baseline brownian motion.

It should be noted that the gaussian distribution is not sharp enough to distinguish between a homogeneous population with a single peak at  $1.3 \text{ nm}$  and a heterogeneous population with a large peak (80% of events) at  $0 \text{ nm}$  and a much smaller peak at  $7.3 \text{ nm}$ . Could 80% of the myosin heads bypass the effective stroke altogether as a result of premature phosphate release, and 20% have a normal stroke size after binding to actin? This model assumes that mutant myosin, unlike the wild type, exists as some myosin-ADP- $\text{P}_i$  (the prestroke state), but primarily as myosin-ADP (the poststroke state, after premature  $\text{P}_i$  release) at the moment of binding to actin. Our calculations on the basis of measured rates and known concentrations show that there is only a small reduction in the steady-state myosin-ADP- $\text{P}_i$  concentration (Table 2) as a result of the increased phosphate-release rate of S456L myosin. It would therefore not be possible to generate heterogeneous populations of myosin molecules that could account for the shift in the gaussian distribution from the changes in phosphate release by the mutant. In fact, there would have to be an almost 300-fold increase in phosphate-release rate to cause a tenfold change in the amount of myosin in the ADP- $\text{P}_i$  state, in which case hydrolysis would be rate-limiting. We examined all steps of the actin-myosin cycle for both

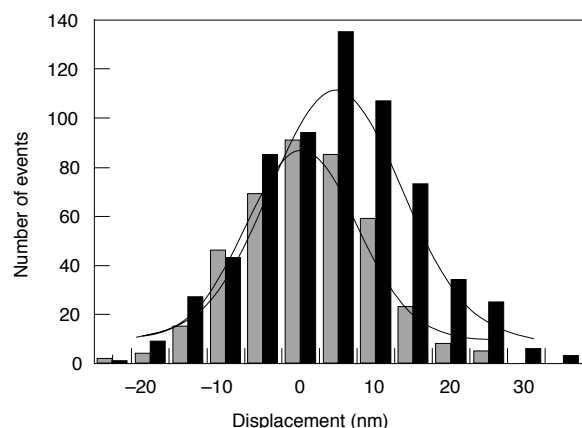


Figure 5 **Measurement of step sizes.** Mean step sizes of wild-type *Dictyostelium* (black) and S456L (grey) myosin are  $7.3 \pm 0.4 \text{ (} n = 640 \text{)}$  and  $1.3 \pm 0.4 \text{ nm (} n = 407 \text{)}$ , respectively. Fits to single gaussian distributions are shown. The step-size measurements shown are uncorrected for system elasticities; we estimate that such correction factors are a maximum of 1.26 for wild-type and 1.33 for mutant myosin<sup>23</sup>.

**Table 1 Wild-type and S456L myosin kinetic activities**

Rate	Wild type	S456L
Basal ATPase (s <sup>-1</sup> )	0.1 ± 0.03	1.0 ± 0.1
ATPase K <sub>m</sub> , ATP (μM)	130 ± 40	510 ± 170
Actin-activated ATPase V <sub>max</sub> , (s <sup>-1</sup> )	2.5 ± 0.5	2.2 ± 0.5
Actin-activated ATPase K <sub>m</sub> , actin (μM)	45 ± 10	n.d.
Hydrolysis rate (s <sup>-1</sup> )*	15.5 ± 0.4	16 ± 0.6
MantADP release from myosin–mantADP (s <sup>-1</sup> )	3.0 ± 0.04	3.0 ± 0.03
MantADP release from actin–myosin–mantADP (s <sup>-1</sup> )	235 ± 11	97 ± 10
ATP co-sedimentation actin affinity (μM)	7.8 ± 4.3	7.9 ± 5.4
Actin–myosin dissociation by ATP (s <sup>-1</sup> )	136 ± 9	141 ± 10

\* The maximum rate of intrinsic tryptophan fluorescence change correlates with the sum of the forward and reverse rates of ATP hydrolysis at saturating Mg<sup>2+</sup>-ATP concentration<sup>29,30</sup>. n.d. not determined; see Fig. 4c.

wild-type and mutant myosin (Fig. 1, Table 1) to eliminate the possibility that an alternative kinetic cycle could account for the observed velocity. Thus, the simplest explanation is that the mutant has a single, shortened step size.

The velocity change as a result of the shortened step size, assuming that  $v = d/t_s$ , would be five- to sixfold. Although the change in step size does not fully account for the observed tenfold reduction in velocity, the combination of these changes in  $d$  and  $t_s$ , as estimated from the twofold change in the rate of ADP release, is in the range that would account for the observed extent of uncoupling. Thus, the uncoupling observed in this Switch II mutant can be explained by a combination of effects on both step size and time spent in the strongly bound state, lending strong support to the model of coupling of chemical energy and mechanical movement proposed for the myosin molecular motor.

We have demonstrated the importance of the ability of myosin to couple the hydrolysis state of ATP to productive interactions with actin, and have shown that a conserved motif in the Switch II region is critical for this coordination. The Switch I and II regions were so named because of the large conformational changes they undergo when bound to different nucleotides, as observed in crystal structures of G proteins<sup>26</sup> and subsequently in myosin structures<sup>4,27</sup>. Perturbation of the Switch II region correlates with a change in the motion of the molecule during its powerstroke, the dynamics of which have been revealed by the laser-trap assay. Energy minimization with a simple potential function of the modelled S456L mutant indicates the occurrence of steric hindrance in the putative ADP–P<sub>i</sub> state (ADP–AlF<sub>4</sub> structure) between the carbonyl group of S237 in Switch I and the leucine at position 456 (Fig. 1b). It is possible that the presence of the larger amino acid prevents the cleft closure that is necessary to generate the full power stroke.

Myosin I has been shown to carry out its working stroke in two steps, the first corresponding to phosphate release and the second to ADP release<sup>28</sup>, and it has been proposed that myosin II may also carry out such a multistep working stroke<sup>28</sup>. Further structural studies will be necessary to determine whether the S456L mutant has only a limited range of motion, or whether it has normal potential but bypasses part of the stroke. It would be extremely interesting to characterize the structure of this state further, to understand the changes that the head and lever arm undergo during the powerstroke. Studying these conformational changes will lead to a better understanding of the way in which motors and other switch-like molecules function. □

**Table 2 Populations of unbound myosins**

	Wild type (%)	S456L (%)
$[M] = \frac{k_3}{k_1[ATP]} [M-D-P_i]$	1 × 10 <sup>-3</sup>	8 × 10 <sup>-3</sup>
$[M-T] = \frac{k_{-2} + k_3}{k_2} [M-D-P_i]$	26.4	25
$[M-D-P_i]$	71	55
$[M-D] = \frac{k_3}{k_4} [M-D-P_i]$	2.5	20



The proportion of myosin (M) in each state can be calculated from the rates, as at steady state the flow into each state equals the flow out and

$M_{total} = [M] + [M-T] + [M-D-P_i] + [M-D]$ . [ATP] = 10 mM;  $k_1 = 7 \times 10^5 \text{ M}^{-1} \text{ s}^{-1}$ ;  $k_2 = 11 \text{ s}^{-1}$ ;  $k_3 = 0.1$  (wild type) or 1.0 (mutant)  $\text{s}^{-1}$ ;  $k_4 = 2.8 \text{ s}^{-1}$ ;  $k_2 = 4 \text{ s}^{-1}$ ;  $k_1, k_3$ , and  $k_4 \approx 0$ . For wild-type myosin, [M-D] + [M-D-P<sub>i</sub>] represents 73.5% of all states, and [M-D-P<sub>i</sub>] represents 96% of the total [M-D] + [M-D-P<sub>i</sub>]. For mutant myosin, [M-D] + [M-D-P<sub>i</sub>] represents 75% of all states, and [M-D-P<sub>i</sub>] represents 72% of the total [M-D] + [M-D-P<sub>i</sub>]. D; ADP, T, ATP.

## Methods

### Reagents.

All reagents were from Sigma. ADP-contaminated ATPγS was purified by degrading the ADP to adenosine and phosphate, using purified alkaline phosphatase (a gift from Patrick O'Brien, Stanford Univ.) and subsequent separation in a Centricon 30 microconcentrator (Amicon, Beverly, Massachusetts). All nucleotide experiments were carried out in buffers containing Mg<sup>2+</sup> in excess of nucleotide.

### Plasmid construction.

Standard methods were used for all DNA manipulations and all restriction enzymes were from New England Biolabs. The HA'20 mutation of the pBIGmyo vector was created as described<sup>6</sup>. The mutagenized plasmid was rescued from cells exhibiting the intermediate developmental phenotype and the entire S1 head was cycle-sequenced to confirm that S456L was the only mutation present.

### Dictyostelium manipulations.

All cells were grown at 22 °C in HL5 or DD-HL5 medium with 100 U ml<sup>-1</sup> penicillin and 100 μg ml<sup>-1</sup> streptomycin. Plasmids were electroporated into HS1, a myosin II-null strain<sup>12</sup>. Transformants were selected for and maintained with 5 μg ml<sup>-1</sup> G418 (Gibco BRL). To monitor growth in suspension, cells were transferred from plates into 100 ml HL5 with penicillin, streptomycin and G418, and allowed to grow for 2 days before being diluted to 5 × 10<sup>4</sup> cells per ml to begin the growth assay. Cells at various densities were developed on lawns of *Klebsiella aerogenes* on SM/5 plates. The pBIGmyo vector expressing wild-type *Dictyostelium* myosin was used as a control in growth and development assays.

### Protein purification.

Myosins were purified as described<sup>5,13</sup> with the addition of a gel-filtration column (Pharmacia Superdex 200 or BioRad Biogel A) to eliminate actin contamination. Myosin was treated with bacterially expressed MLCK-A with the activating point mutation T166E (ref. 14). Myosin concentrations were determined by Bradford assay using rabbit skeletal myosin as a standard<sup>15</sup>. All assays were carried out on at least three preparations of myosin and are reported as means ± s.d.

Actin was purified from chicken skeletal muscle as described<sup>16</sup>. Actin was labelled with N-(1-pyrene)iodoacetamide (Molecular Probes) as described<sup>17</sup>. Phalloidin (Sigma) was added in 5:1 molar excess to actin to stabilize the filaments for all stopped-flow and spectrophotometry experiments.

### ATPase assays.

Myosin ATPase activities at 30 °C were determined by measuring release of labelled P<sub>i</sub> using [<sup>32</sup>P]ATP as previously described<sup>18</sup>. Reactions contained 25 mM imidazole pH 7.4, 25 mM KCl, 4 mM MgCl<sub>2</sub>, 1 mM dithiothreitol (DTT) and varying concentrations of ATP and actin; 3 mM ATP was used in the actin-activated ATPase assays. Curves were fitted to the Michaelis–Menten equation in KaleidaGraph (Abelbeck Software, Reading, Pennsylvania).

### In vitro motility assays.

After removing MLCK-A-treated myosin that is unable to be dissociated from actin by ATP, motility was measured using standard sliding-filament assay methods at 30 °C (refs 13, 20). Myosin (0.06–0.8 mg ml<sup>-1</sup>) was applied to the flow cell in high-salt assay buffer (HSAB; 25 mM imidazole pH 7.4, 300 mM KCl, 1 mM EGTA and 10 mM DTT) and assayed for movement in low-salt (25 mM KCl) assay buffer containing 10 mM Mg<sup>2+</sup>-ATP, 1 mg ml<sup>-1</sup> BSA and an oxygen scavenger system, in the presence or absence of 0.8% methylcellulose. Actin filaments were monitored using a frame-grabber board (Scion

Corp, Frederick, Maryland) and images were processed using NIH Image as described<sup>13,19</sup>.

### Co-sedimentation assays.

G-actin was treated with gelsolin at a ratio of 1 gelsolin molecule to 20 actin monomers, and was then polymerized by addition of KCl (to 25 mM), MgCl<sub>2</sub> (to 3 mM) and ATP (to 2 mM). Polymerized actin was added in increasing amounts (4–36 μM) to 1 μM myosin and the mixture was centrifuged at 3,500g in the presence of 3 mM ATP or 3 mM ATPγS in ATPase buffer. Under these conditions, filamentous myosin is pelleted but gelsolin-treated actin remains primarily in the supernatant. Pellets were resuspended and subjected to SDS-PAGE; Coomassie blue-stained gels were analysed using the AlphaImager 2000 system (AlphaInnotech Corp., San Leandro, California). For each actin concentration, a zero-myosin point was subtracted as a control for baseline actin pelleting. Densities were normalized according to an actin standard curve and the known concentration of myosin in each lane, and were used to determine the  $K_d$  by curve-fitting in KaleidaGraph ( $[\text{actin}]_{\text{bound}}/[\text{myosin}]$  relative to  $[\text{actin}]_{\text{initial}}$ ; ref. 18).

### Stopped-flow spectrophotometry.

Stopped-flow experiments were carried out as described<sup>13,18</sup> at 20 °C in a standard buffer (25 mM HEPES pH 7.4, 1 mM DTT, 5 mM MgCl<sub>2</sub> and 25 mM KCl). Light was provided by a mercury-xenon lamp (Hamamatsu) and was passed through an Applied Photophysics SpectraKinetic monochromator; a DX.17MV Sequential Stopped-flow Spectrophotometer (Applied Photophysics, Leatherhead, UK) was used. For each protein preparation, at least four superimposable runs were carried out for each experiment. Data were analysed by a least-squares fitting procedure (Kaleidagraph) and are expressed as means ± s.d. Experiments requiring saturating ATP concentrations were carried out at both 10 and 25 mM Mg<sup>2+</sup>-ATP.

### Optical-trap assays.

Surface-bound silica spheres were decorated sparsely with myosin II introduced into the cell at 20 μg ml<sup>-1</sup>. Flow cells were constructed and assays were carried out and analysed as described<sup>22–25</sup>. Assays were carried out in 25 mM imidazole-HCl pH 7.4, 25 mM KCl, 1 mM EGTA, 10 mM DTT, 4 mM Mg<sup>2+</sup>-ATP, and an oxygen scavenger system (25 μg ml<sup>-1</sup> glucose oxidase, 45 μg ml<sup>-1</sup> catalase and 1% (w/v) glucose) at 23 °C. The stiffness of each trap was 0.03 pN nm<sup>-1</sup>. Step sizes are expressed as means ± s.e.m. The measured times spent in the strongly bound state at limiting ATP concentration may be fitted by a single exponential (with a lifetime consistent with the second-order ATP-association rate), indicating that a single myosin molecule is responsible for the measured values.

RECEIVED 24 JULY 2000; REVISED 4 OCTOBER 2000; ACCEPTED 30 OCTOBER 2000;  
PUBLISHED 16 FEBRUARY 2001.

1. Goldman, Y. E. *Cell* **93**, 1–4 (1998).
2. Vale, R. D. *J. Cell Biol.* **135**, 291–302 (1996).

3. Sellers, J. R. & Goodson, H. V. in *Motor proteins 2: Myosin* (ed. Shterline, P.) (Academic, London, 1995).
4. Fisher, A. J. *et al. Biochemistry* **34**, 8960–8972 (1995).
5. Ruppel, K. M. & Spudich, J. A. *Mol. Biol. Cell* **7**, 1123–1136 (1996).
6. Sasaki, N., Shimada, T. & Sutoh, K. *J. Biol. Chem.* **273**, 20334–20340 (1998).
7. Furch, M., Fujita-Becker, S., Geeves, M. A., Holmes, K. C. & Manstein, D. J. *J. Mol. Biol.* **290**, 797–809 (1999).
8. Li, X. D. *et al. J. Biol. Chem.* **273**, 27404–27411 (1998).
9. Kambara, T. *et al. J. Biol. Chem.* **274**, 16400–16406 (1999).
10. Onishi, H. *et al. Proc. Natl Acad. Sci. USA* **95**, 6653–6658 (1998).
11. Springer, M. L., Patterson, B. & Spudich, J. A. *Development* **120**, 2651–2660 (1994).
12. Manstein, D. J., Titus, M. A., De Lozanne, A. & Spudich, J. A. *EMBO J.* **8**, 923–932 (1989).
13. Murphy, C. T. & Spudich, J. A. *Biochemistry* **37**, 6738–6744 (1998).
14. Smith, J. L., Silveira, L. A. & Spudich, J. A. *EMBO J.* **15**, 6075–6083 (1996).
15. Bradford, M. M. *Anal. Biochem.* **72**, 248–254 (1976).
16. Pardee, J. D. & Spudich, J. A. *Methods Cell Biol.* **24**, 271–289 (1982).
17. Criddle, A. H., Geeves, M. A. & Jeffries, T. *Biochemistry* **232**, 343–349 (1985).
18. Murphy, C. T. & Spudich, J. A. *Biochemistry* **38**, 3785–3792 (1999).
19. Marriott, G. & Heidecker, M. *Biochemistry* **35**, 3170–3174 (1996).
20. Kron, S. J. & Spudich, J. A. *Proc. Natl Acad. Sci. USA* **83**, 6272–6276 (1986).
21. Spudich, J. A. *Nature* **372**, 515–518 (1994).
22. Siemankowski, R. F., Wiseman, M. O. & White, H. D. *Proc. Natl Acad. Sci. USA* **82**, 658–662 (1985).
23. Mehta, A. D., Finer, J. T. & Spudich, J. A. *Proc. Natl Acad. Sci. USA* **94**, 7927–7931 (1997).
24. Mehta, A. D. *et al. Nature* **400**, 590–593 (1999).
25. Mehta, A. D., Finer, J. T., Spudich, J. A. *Methods Enzymol.* **298**, 436–459 (1998).
26. Kjeldgaard, M., Nissen, P., Thirup, S. & Nyborg, J. *Structure* **1**, 35–50 (1993).
27. Dominguez, R., Freyzon, Y., Trybus, K. M. & Cohen, C. *Cell* **94**, 559–571 (1998).
28. Veigel, C. *et al. Nature* **398**, 530–533 (1999).
29. Ritchie, M. D., Geeves, M. A., Woodward, S. K. A. & Manstein, D. J. *Proc. Natl Acad. Sci. USA* **90**, 8619–8623 (1993).
30. Bauer, C. B., Kuhlman, P. A., Bagshaw, C. R. & Rayment, I. *J. Mol. Biol.* **274**, 394–707 (1997).

### ACKNOWLEDGEMENTS

We thank A. Mehta for the wild type step size data and H. Warrick, D. Robinson and D. Hostetter for comments. C.T.M. was a Predoctoral Fellow of the Howard Hughes Medical Institute. R.S.R. is a Helen Hay Whitney Fellow.

Correspondence and requests for materials should be addressed to J.A.S.